Phosphoantigen sensing combines TCR-dependent recognition of the BTN3A IgV domain and germline interaction with BTN2A1

Willcox, Carrie R; Salim, Mahboob; Begley, Charlotte R; Karunakaran, Mohindar M; Easton, Emily J; von Klopotek, Carlotta; Berwick, Katie A; Herrmann, Thomas; Mohammed, Fiyaz; Jeeves, Mark; Willcox, Benjamin E

DOI:
10.1016/j.celrep.2023.112321

Document Version
Publisher's PDF, also known as Version of record

Citation for published version (Harvard):
Willcox, CR, Salim, M, Begley, CR, Karunakaran, MM, Easton, EJ, von Klopotek, C, Berwick, KA, Herrmann, T, Mohammed, F, Jeeves, M & Willcox, BE 2023, 'Phosphoantigen sensing combines TCR-dependent recognition of the BTN3A IgV domain and germline interaction with BTN2A1', *Cell Reports*, vol. 42, no. 4, 112321. https://doi.org/10.1016/j.celrep.2023.112321

Cell Reports

Phosphoantigen sensing combines TCR-dependent recognition of the BTN3A IgV domain and germline interaction with BTN2A1

Graphical abstract

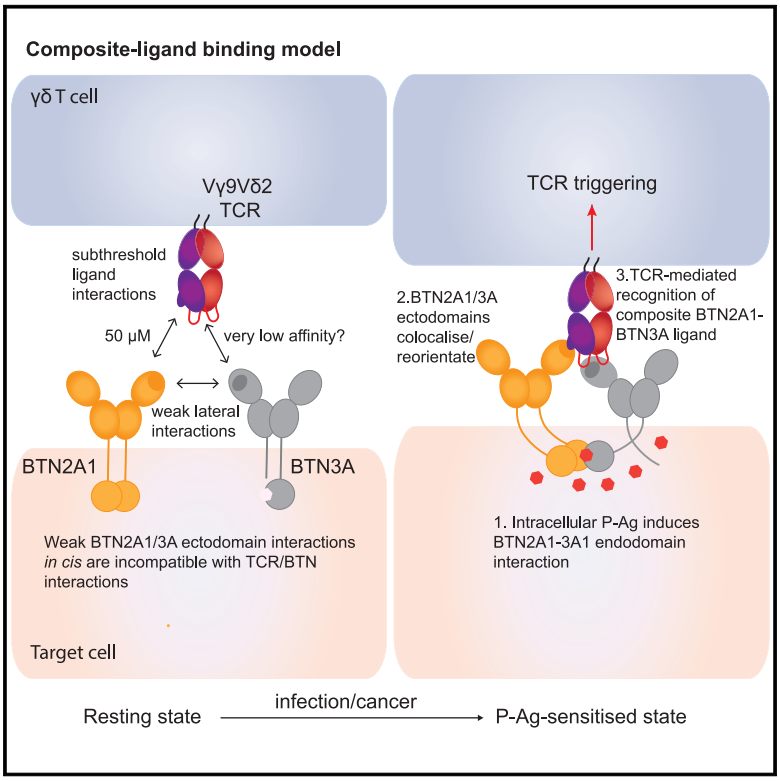

Highlights

- Molecular approaches predict cell-surface BTN2A1-IgV/BTN3A1-IgV interaction in *cis*
- Vγ9Vδ2 TCR binding to BTN2A1 is incompatible with BTN2A1-IgV/BTN3A1-IgV interaction
- BTN2A1-IgV/BTN3A1-IgV interaction is dispensable for phosphoantigen (P-Ag) sensing
- Mutagenesis reveals a BTN3A-IgV "antigenic hotspot" critical for T cell activation

Authors

Carrie R. Willcox, Mahboob Salim, Charlotte R. Begley, ..., Fiyaz Mohammed, Mark Jeeves, Benjamin E. Willcox

Correspondence

c.r.willcox@bham.ac.uk (C.R.W.), m.jeeves@bham.ac.uk (M.J.), b.willcox@bham.ac.uk (B.E.W.)

In brief

Willcox et al. model the BTN2A1-IgV/BTN3A1-IgV interaction in *cis*, highlight incompatibility with the Vγ9Vδ2 TCR/BTN2A1 interaction, and identify a critical antigenic hotspot on BTN3A-IgV. These data support a "composite-ligand" phosphoantigen (PAg)-sensing model whereby intracellular P-Ag detection coordinates simultaneous weak TCR-mediated recognition of BTN2A1 and BTN3A1 to achieve Vγ9Vδ2 TCR triggering.

Willcox et al., 2023, Cell Reports *42*, 112321
April 25, 2023
https://doi.org/10.1016/j.celrep.2023.112321

CellPress

Cell Reports

CellPress
OPEN ACCESS

Report

Phosphoantigen sensing combines TCR-dependent recognition of the BTN3A IgV domain and germline interaction with BTN2A1

Carrie R. Willcox,[1,2,5,*] Mahboob Salim,[1,2,5] Charlotte R. Begley,[1,2] Mohindar M. Karunakaran,[3] Emily J. Easton,[1,2] Carlotta von Klopotek,[3] Katie A. Berwick,[1,2] Thomas Herrmann,[3] Fiyaz Mohammed,[1,2,5] Mark Jeeves,[4,5,*] and Benjamin E. Willcox[1,2,5,6,*]

[1]Institute of Immunology and Immunotherapy, University of Birmingham, Birmingham, UK
[2]Cancer Immunology and Immunotherapy Centre, University of Birmingham, Birmingham, UK
[3]Institute for Virology and Immunobiology, University of Würzburg, Würzburg, Germany
[4]Henry Wellcome Building for NMR, Institute of Cancer and Genomic Sciences, University of Birmingham, Birmingham, UK
[5]These authors contributed equally
[6]Lead contact
*Correspondence: c.r.willcox@bham.ac.uk (C.R.W.), m.jeeves@bham.ac.uk (M.J.), b.willcox@bham.ac.uk (B.E.W.)
https://doi.org/10.1016/j.celrep.2023.112321

SUMMARY

Vγ9Vδ2 T cells play critical roles in microbial immunity by detecting target cells exposed to pathogen-derived phosphoantigens (P-Ags). Target cell expression of BTN3A1, the "P-Ag sensor," and BTN2A1, a direct ligand for T cell receptor (TCR) Vγ9, is essential for this process; however, the molecular mechanisms involved are unclear. Here, we characterize BTN2A1 interactions with Vγ9Vδ2 TCR and BTN3A1. Nuclear magnetic resonance (NMR), modeling, and mutagenesis establish a BTN2A1-immunoglobulin V (IgV)/BTN3A1-IgV structural model compatible with their cell-surface association in *cis*. However, TCR and BTN3A1-IgV binding to BTN2A1-IgV is mutually exclusive, owing to binding site proximity and overlap. Moreover, mutagenesis indicates that the BTN2A1-IgV/BTN3A1-IgV interaction is non-essential for recognition but instead identifies a molecular surface on BTN3A1-IgV essential to P-Ag sensing. These results establish a critical role for BTN3A-IgV in P-Ag sensing, in mediating direct or indirect interactions with the γδ-TCR. They support a composite-ligand model whereby intracellular P-Ag detection coordinates weak extracellular germline TCR/BTN2A1 and clonotypically influenced TCR/BTN3A-mediated interactions to initiate Vγ9Vδ2 TCR triggering.

INTRODUCTION

Vγ9Vδ2 T cells make unique contributions to antimicrobial immunity in higher mammals by recognizing target cells exposed to non-peptidic phosphoantigens (P-Ags),[1,2] including the highly potent (*E*)-4-Hydroxy-3-methyl-but-2-enyl pyrophosphate (HMBPP) antigen derived from the microbial-specific non-mevalonate pathway of isoprenoid biosynthesis.[3] Following exogenous P-Ag detection, they mount major histocompatibility complex (MHC)-independent effector responses to pathogens of major clinical importance,[4] including cytotoxicity and cytokine production[2,5]; they are also capable of phagocytosis of opsonized target cells.[5] However, in addition to detection of microbial P-Ags, Vγ9Vδ2 T cells also respond to IPP, a less potent P-Ag, which derives from the mammalian mevalonate pathway that can be naturally upregulated or pharmacologically targeted in cancer cells.[2] Aligned with this, the subset is a focus of considerable therapeutic development in the context of cancer immunotherapy. The molecular mechanisms involved in P-Ag recognition are therefore of substantial interest. Butyrophilin family molecules have emerged as central players in this process—with target cell expression of BTN3A1[6] and, more recently, BTN2A1[7,8] established as essential to P-Ag sensing. Determining how P-Ag sensing occurs is arguably core to understanding Vγ9Vδ2 T cell biology, may have wider implications for other γδ T cell subsets where BTN family members have been implicated in their immunobiology,[9,10] and could open up new opportunities for therapeutic manipulation of this universal human T cell population.

BTN2A1 and BTN3A1 clearly play highly distinct roles in Vγ9Vδ2 T cell detection of P-Ag-exposed cells. BTN3A1 acts as the intracellular "P-Ag sensor"[11] by binding P-Ags in the cytosol, which triggers conformational changes in its intracellular B30.2 domain.[11–15] In contrast, BTN2A1 was recently identified by our own group[7] and others[8] as a direct ligand for TCR Vγ9 via a low-affinity (50 μM) binding mode restricted to germline-encoded T cell receptor (TCR) elements including the HV4 region. However, although this interaction is a critical requirement for P-Ag reactivity, other regions of the TCR are vital for P-Ag sensing, notably including the CDR3δ and CDR3γ regions.[16] Moreover, our previous modeling of the Vγ9Vδ2 TCR interaction with BTN2A1 indicated recognition of the BTN2A1 CC'FG (CFG)

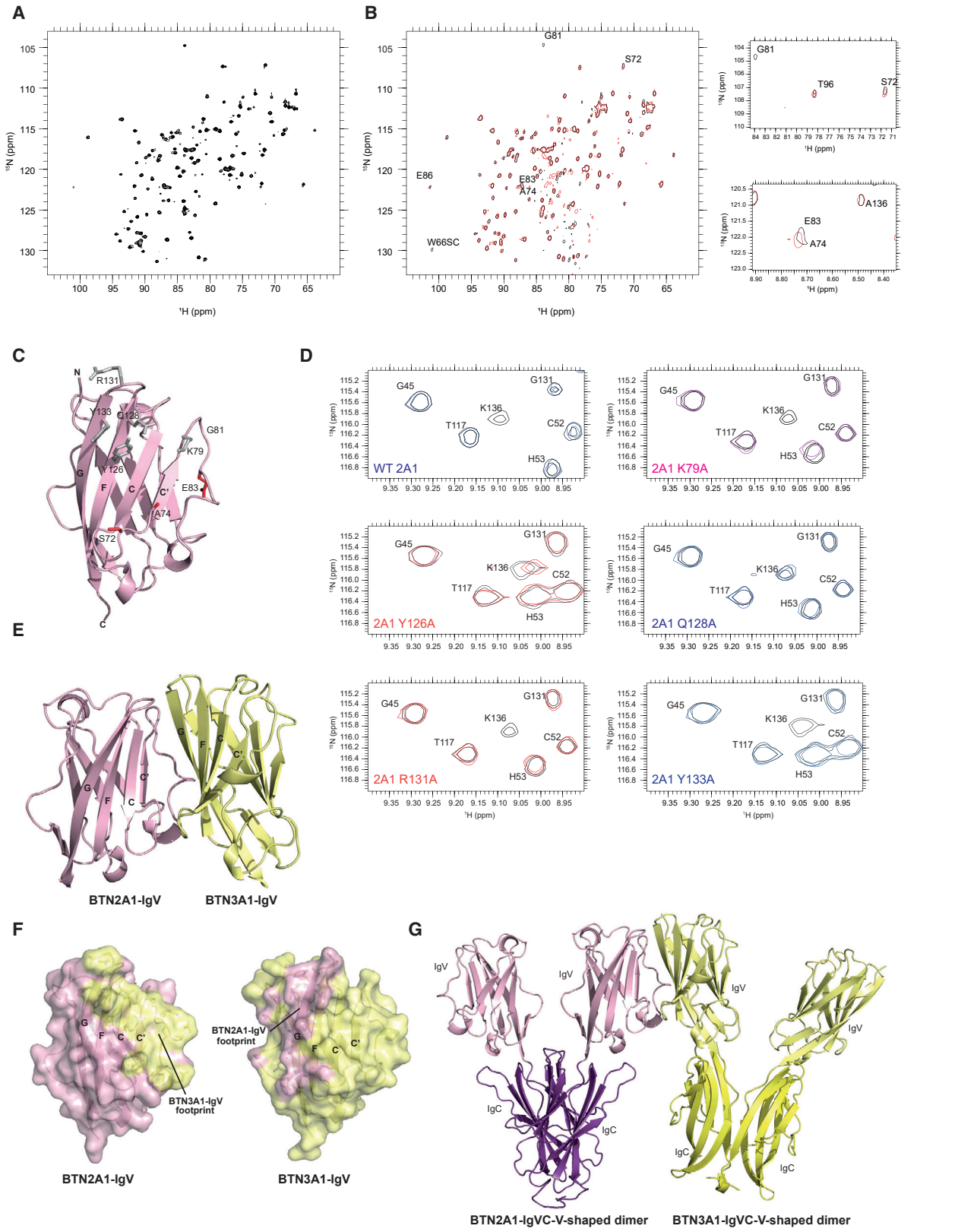

(legend on next page)

face by the lateral, germline-encoded surface of the TCR Vγ9 chain, leaving the membrane-distal surface comprising other CDR loops also implicated in P-Ag sensing (CDR1γ, CDR3γ, CDR1δ, CDR2δ, CDR3δ) available for additional interactions.[7] Collectively, this clearly suggests that other CDR-recognized TCR ligands are likely involved in Vγ9Vδ2 TCR triggering.

How BTN3A1 and BTN2A1 functionality becomes coupled in the presence of P-Ag is currently unclear. Both the nature of the P-Ag-induced changes communicated to the TCR, and also how this communication occurs, is currently ill defined. An important recent study showed that P-Ag binding to the BTN3A1 B30.2 domain induces association with the BTN2A1 B30.2 region[17] and that it could be a proximal consequence of intracellular P-Ag detection. However, the extracellular recognition events involving BTN2A1, BTN3A1, and TCR that occur following P-Ag detection are less clear. Of relevance, we previously showed that the membrane-distal immunoglobulin V (IgV) domains of BTN2A1 and BTN3A1 can directly interact.[7] This raised the question of whether such BTN3A1-IgV/BTN2A1-IgV interactions are essential for P-Ag sensing and contribute to the Vγ9Vδ2 TCR recognition complex following intracellular P-Ag exposure.[7]

Here, we shed light on extracellular recognition events central to P-Ag sensing by employing a range of molecular approaches to define the nature of the BTN2A1-IgV/BTN3A1-IgV interaction, its significance in P-Ag sensing, and the importance of the BTN3A1-IgV domain. The results support a composite-ligand model of P-Ag sensing whereby intracellular P-Ag detection induces assembly of a heteromeric butyrophilin ligand complex permitting simultaneous germline TCR interaction with BTN2A1 alongside parallel TCR-mediated recognition of BTN3A.

RESULTS

Molecular modeling of BTN2A1/BTN3A1 interaction

Having established that BTN2A1 not only represents a direct ligand for a canonical Vγ9Vδ2 TCR but can also interact with the P-Ag sensor BTN3A1 via its ectodomain,[7] we first aimed to determine the binding mode for this interaction. Previously, using nuclear magnetic resonance (NMR), we were able to detect binding of wild-type (WT) BTN2A1-IgV to ^{15}N-^{13}C-labeled BTN3A1-IgV, confirming a low-affinity interaction (K_d >100 μM) and enabling mapping of residues on BTN3A1 that were involved, which we observed were clustered on the CFG face of the domain.[7] To determine the region of BTN2A1-IgV involved in the interaction, we first collected a heteronuclear single quantum coherence (HSQC) spectrum of ^{15}N-labeled BTN2A1 (Figure 1A). Sequence-specific assignments were achieved using ^{15}N-^{13}C-labeled protein, resulting in the backbone amide assignment of 102 out of 113 non-proline residues. For the remaining residues, signal overlap and internal conformational exchange meant that unambiguous assignment was not possible. Subsequent addition of unlabeled BTN3A1-IgV resulted in the perturbation or disappearance of several resonances assigned to specific BTN2A1-IgV residues (Figures 1B and S1A), including S72, A74, G81, and E83, which are located on the CFG face (Figure 1C). The perturbations seen are in fast exchange with small chemical shift changes, with the disappearance of peaks being due to those residues being in intermediate exchange because of the larger chemical shift difference between the resonances of the bound and free forms. This, together with the low number of residues affected, suggests that the interaction is relatively weak with a small contact interface. Mapping these onto the BTN2A1-IgV surface, we were able to highlight several additional nearby residues as candidates for involvement, namely K79, Y126, Q128, R131, and Y133 (Figure 1C). The addition of unlabeled BTN2A1-IgV bearing single alanine mutations at these residues to ^{15}N-labeled BTN3A1-IgV (Figures 1D and S1B) indicated that two of these residues negatively impacted BTN3A1 interaction: Q128A eliminated BTN3A1 binding completely, and Y126A altered it; in contrast, K79A, R131A, and Y133A did not impact the BTN3A1-IgV interaction. This was clearly seen in the disappearance of the signal for BTN3A1 residue K136 upon addition of BTN2A1-IgV mutants K79A, R131A, and Y133A, matching the effect seen upon addition of WT-BTN2A1-IgV, while the addition of BTN2A1 Q128A resulted in no changes to the spectrum of BTN3A1-IgV, indicating no binding, and BTN2A1 Y126A caused only a small perturbation, suggesting altered binding (Figure 1D). This is further corroborated when examining the effect on BTN3A1 residue V68, which showed differential shifting dependent on the mutant of BTN2A1-IgV used (Figure S1B). We then applied our previous mutation-/NMR-informed molecular docking approach[7] to generate a model of the BTN2A1-IgV/BTN3A1-IgV interaction using the HADDOCK program[18,19] (Figures 1E and 1F). The binding mode was consistent with BTN2A1 and BTN3A1 protruding

Figure 1. Modeling the BTN2A1-BTN3A1 ectodomain interaction

(A) ^{1}H-^{15}N-HSQC spectrum of 750 μM ^{15}N-^{13}C-labeled BTN2A1-IgV.

(B) Overlay of ^{1}H-^{15}N-HSQC spectra of 80 μM ^{15}N-^{13}C-labeled BTN2A1-IgV (black) with 80 μM ^{15}N-^{13}C-labeled BTN2A1-IgV plus 400 μM unlabeled BTN3A1-IgV (red). Residues that show significant chemical shift perturbations and those that show dramatic line broadening due to being in intermediate exchange are labeled and shown in insets.

(C) Ribbon representation of the BTN2A1-IgV domain. BTN2A1 residues with chemical-shift perturbations upon BTN3A1 binding are mapped (red), plus other candidate mutations (gray).

(D) Overlay of the ^{1}H-^{15}N-HSQC spectrum of 250 μM ^{15}N-labeled BTN3A1-IgV (black), with 250 μM ^{15}N-labeled BTN3A1-IgV after the addition of 250 μM of WT and different mutants of BTN2A1-IgV (colored as indicated). Most resonances of BTN3A1-IgV are unaffected, but some (highlighted here by K136) show significant line broadening consistent with being in intermediate chemical exchange leading to the loss of signal. Mutants of BTN2A1-IgV cause varying effects on the ^{1}H-^{15}N-HSQC spectrum of BTN3A1-IgV suggesting differential binding effects.

(E) HADDOCK derived model of the BTN2A1-IgV/BTN3A1-IgV complex.

(F) Molecular surface representation of the BTN2A1-IgV (pink) and BTN3A1-IgV (yellow) domains. The putative binding footprints are highlighted on each surface.

(G) Full V-shaped BTN3A1-BTN2A1 ectodomain interaction extrapolated from the BTN2A1-IgV/BTN3A1-IgV model.

See also Figure S1.

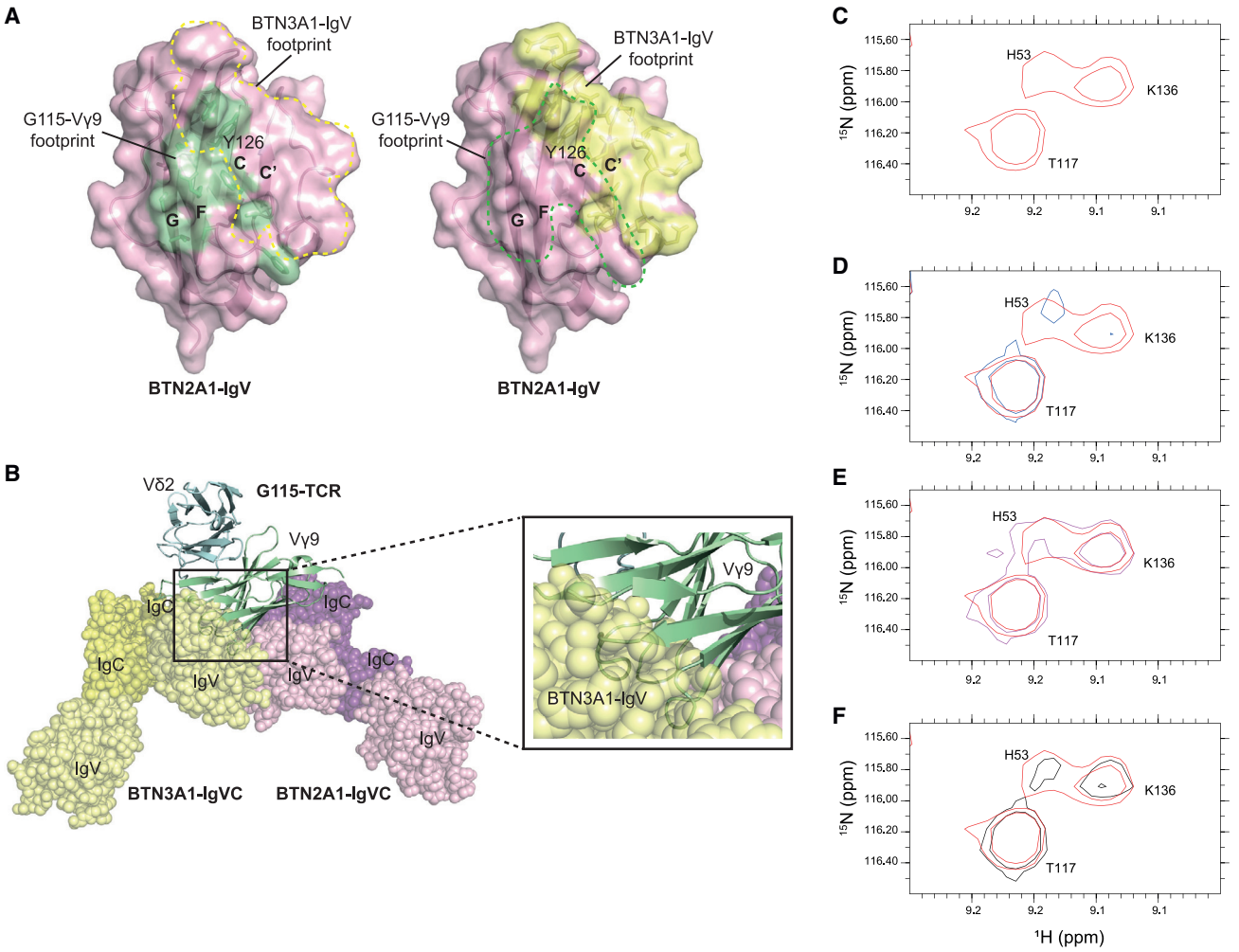

Figure 2. TCR binding BTN2A1 prevents formation of a TCR/BTN2A1-BTN3A1 complex

(A) Molecular surface representation of BTN2A1-IgV (pink), with the BTN3A1-IgV (yellow) and G115-Vγ9 (green) binding footprints mapped.

(B) Predicted model of the BTN2A1/BTN3A1/G115 triple complex. The G115-Vγ9 domain clashes with the BTN3A1-IgV domain. The V-shaped BTN2A1 and BTN3A1 ectodomains are shown as spheres. The constant domains for the G115-TCR have been omitted for clarity.

(C–F) Region of the ^{1}H-^{15}N-HSQC spectrum of 100 μM ^{15}N-labeled BTN3A1-IgV (C) focusing in on residues H53, K136, and T117 (red). Overlay of a region of the spectrum of 100 μM ^{15}N-labeled BTN3A1-IgV (red) with a spectrum of 100 μM ^{15}N-labeled BTN3A1-IgV after the addition of 100 μM BTN2A1-IgV (D, blue), 100 μM G115 TCR (E, purple), and 100 μM each of BTN2A1-IgV and G115 TCR (F, black).

See also Figure S2.

from the same cell membrane with the long axis of each dimer approximately in parallel, indicative of a plausible in *cis* interaction mode on the target cell surface (Figure 1G).

TCR binding to BTN2A1 precludes BTN2A1/BTN3A1 interaction

We next addressed whether the Vγ9Vδ2 TCR was able to directly engage a BTN2A1-IgV/BTN3A1-IgV complex. Comparison of the binding surfaces of BTN2A1-IgV predicted to be involved in interaction with either TCR (Figure S2A) or BTN3A1 indicated use of the same outer CFG face of the domain and highlighted substantial overlap (Figure 2A). Moreover, superimposition of molecular models of BTN2A1-IgV interactions with each protein highlighted major steric clashes between the TCR and BTN3A1 (Figure 2B). In addition, BTN2A1-IgV Y126A mutation negatively impacted both Vγ9Vδ2 TCR binding[7] and BTN3A1 interaction (Figure 1), suggesting potential overlap in both binding footprints. Based on these collective data, we predicted that a triple complex of TCR binding to the BTN3A1-IgV/BTN2A1-IgV in *cis* heterodimer was unlikely to occur.

To directly address this prediction, we assessed whether binding of unlabeled BTN2A1-IgV to ^{15}N-labeled BTN3A1-IgV, readily detectable by NMR, was influenced by the presence of unlabeled Vγ9Vδ2 TCR. Addition of unlabeled BTN2A1-IgV induced chemical shifts in BTN3A1-IgV residues we had previously identified as being involved in BTN2A1 interactions (including K136) (Figures 2C and 2D). In contrast, unlabeled Vγ9Vδ2 TCR produced no shifts when added to ^{15}N-labeled

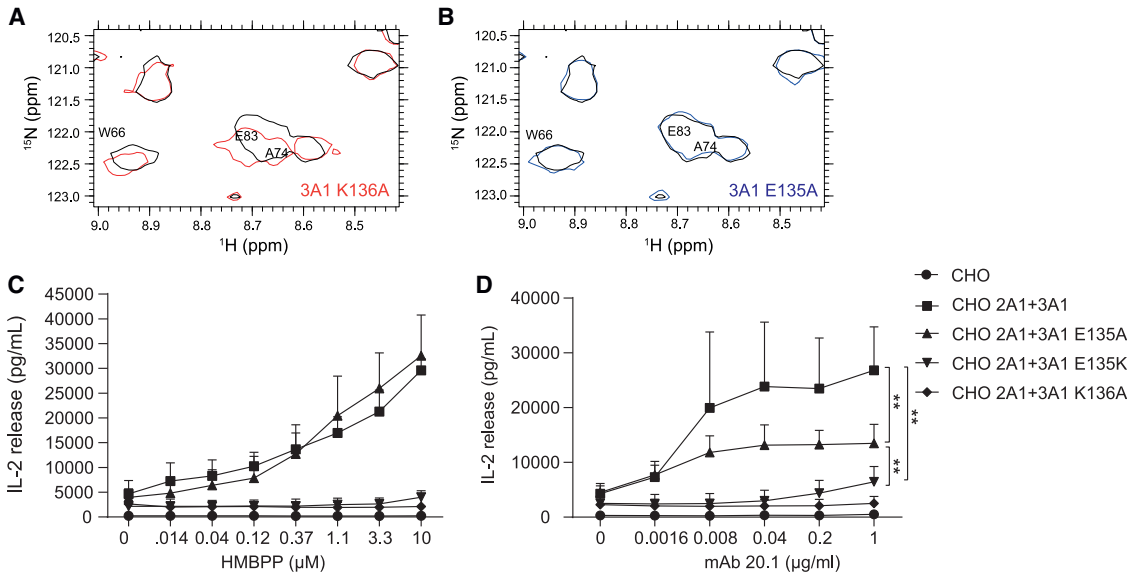

Figure 3. BTN2A1-IgV interaction with BTN3A1-IgV is not required for P-Ag sensing

(A) Overlay of a region of the ^{1}H-^{15}N-HSQC spectrum of 100 μM ^{15}N-labeled WT BTN2A1-IgV (black) with a ^{1}H-^{15}N-HSQC spectrum of 100 μM ^{15}N-labeled WT BTN2A1-IgV after addition of 100 μM BTN3A1-IgV K136A mutant (red).

(B) As for (A) but after addition of 100 μM BTN3A1-IgV E135A mutant (blue).

(C and D) Interleukin-2 (IL-2) production by MOP TCR hybridoma cells in response to CHO cells expressing BTN2A1 and WT or the indicated mutant BTN3A1 following HMBPP treatment (C) or treatment with 20.1 mAb (D) at the indicated concentrations. Shown are mean ± SD of three independent experiments. **$p < 0.005$; two-way ANOVA.

See also Figure S3.

BTN3A1-IgV, confirming the lack of a detectable Vγ9Vδ2 TCR/BTN3A1 interaction at the concentrations used (Figures 2E and S2B). Due to its relatively large size (>60 kDa), binding of the TCR to an in *cis* BTN2A1-BTN3A1 heterodimer complex would be expected to cause significant broadening and lead to the loss of detectable signal from ^{15}N-labeled BTN3A1. However, the addition of Vγ9Vδ2 TCR alongside BTN2A1-IgV resulted in the loss of any BTN2A1-IgV-induced shifts in ^{15}N-BTN3A1-IgV residues but restored and maintained resonances from unliganded ^{15}N-BTN3A1 (Figure 2F). These data provide objective quantitative evidence that Vγ9Vδ2 TCR binding to BTN2A1 precludes interaction of the latter protein with BTN3A1 and confirms that a "triple complex" involving a TCR interaction with a BTN2A1-IgV/BTN3A1-IgV in *cis* heterodimer is biochemically unfeasible. In addition, restoration and maintenance of resonances from unliganded ^{15}N-BTN3A1-IgV after the addition of TCR excludes the possibility that TCR binding to BTN2A1-IgV leads to a conformational change in either protein that promotes interaction with BTN3A1-IgV or, alternatively, that BTN2A1-IgV/BTN3A1-IgV alters BTN3A1-IgV conformation in such a way as to promote TCR binding.

BTN2A1-IgV interaction with BTN3A1-IgV is redundant for P-Ag sensing

We next sought to assess directly the functional importance of the BTN2A1-IgV/BTN3A1-IgV interaction for Vγ9Vδ2 T cell recognition. Previously, we noted that the K136M (along with Y127W and R73H) mutation on BTN3A1/3A2-IgV eliminated P-Ag sensing[20]; however, whether this had effects on BTN2A1-IgV interactions was unclear. To address this concept, we assessed in parallel the effects of specific mutations on both BTN2A1-IgV/BTN3A1-IgV association and on P-Ag sensing, the latter exploiting an established CHO cell assay system that expressed single human BTN2 and BTN3 genes (BTN2A1 and BTN3A1 respectively), thereby eliminating potential redundancy in BTN3A1/3A2/3A3 isoforms in some human systems.[7,20]

Two BTN3A1-IgV mutants were especially informative (Figures 3A and 3B). The BTN3A1 E135A mutant eliminated interaction with ^{15}N-BTN2A1 completely as assessed via NMR but completely retained the ability to synergize with WT BTN2A1 in CHO cell assays to mediate HMBPP-induced activation of the 53/4 hybridoma line expressing the MOP Vγ9Vδ2 TCR (Figure 3C). In contrast, a second BTN3A1-IgV mutant, K136A, was found to bind to BTN2A1-IgV equivalently to WT BTN3A1-IgV in NMR (Figure 3A) but completely abrogated P-Ag sensing by the MOP T cell hybridoma (Figure 3C), consistent with previous findings.[20] Complementary NMR studies carried out using ^{15}N-labeled BTN3A1 mutants and unlabeled WT BTN2A1-IgV (Figures S3A and S3B) corroborated the effects of these mutations on BTN2A1-IgV interactions. Of note, the effects of these mutations on 20.1 monoclonal antibody (mAb)-mediated activation (Figure 3D) largely mirrored those on HMBPP-induced activation in that the K136A mutation abrogated activity, whereas the E135A mutant permitted 20.1 mAb-mediated activation. However, for E135A, functionality was not fully retained relative to WT BTN3A1, suggesting that HMBPP and 20.1 mAb-mediated activation are not completely equivalent. These results indicated that, at least in the CHO cell system we used, direct

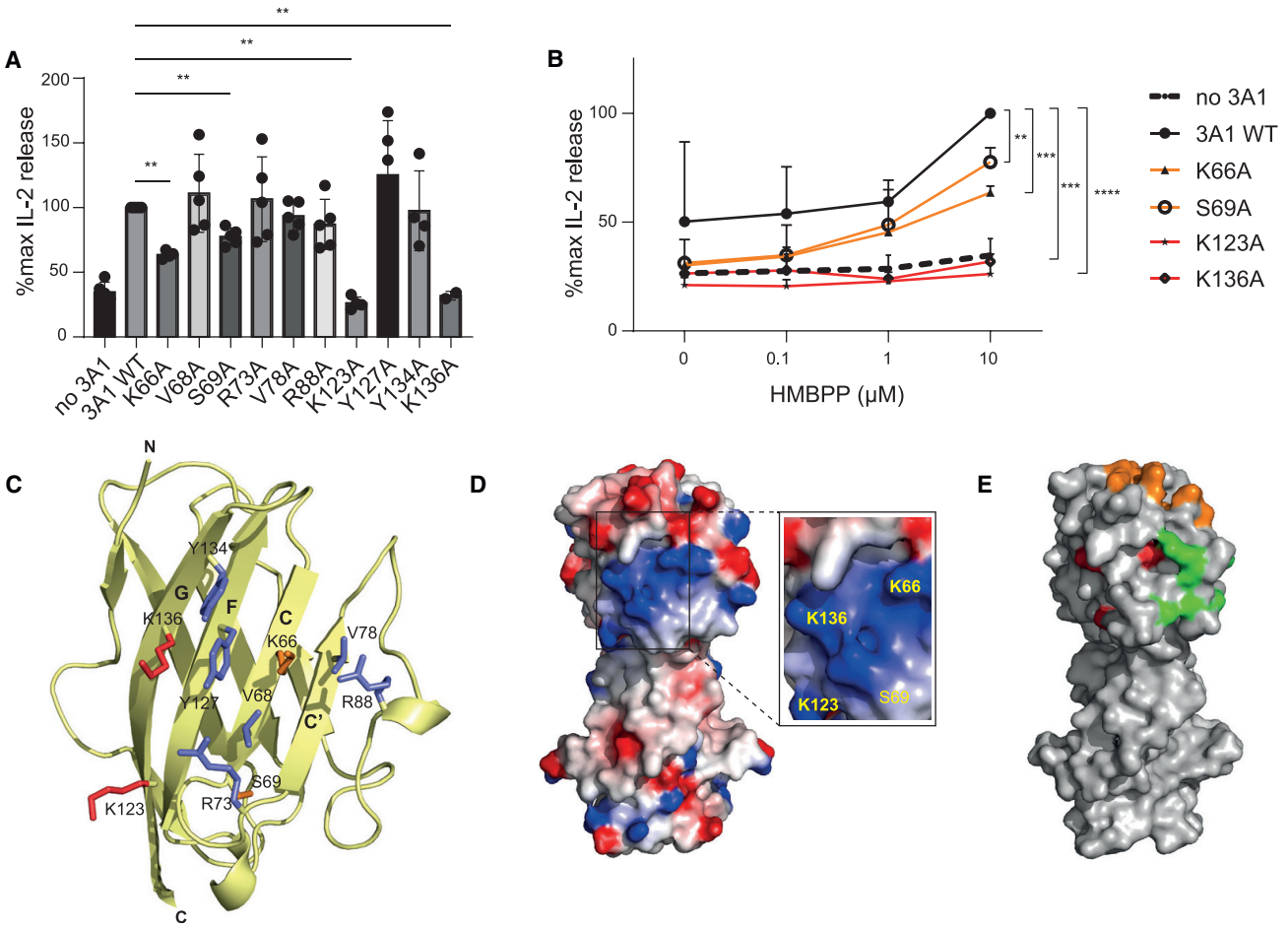

Figure 4. Identification of a surface patch on BTN3A1-IgV critical for P-Ag sensing

(A) IL-2 production by MOP TCR hybridoma cells in response to CHO cells expressing BTN2A1 and WT or mutant BTN3A1 following HMBPP treatment at 10 μM. Data are shown as mean ± SD of 3–5 experiments per mutant cell line. **p < 0.005; Mann-Whitney.

(B) IL-2 production by MOP TCR hybridoma cells in response to CHO cells expressing BTN2A1 and WT or mutant BTN3A1, treated with HMBPP at the indicated concentration. Activation is given as percentage of activation observed with CHO cells expressing BTN3A1 WT at 10 μM HMBPP in the same experiment. Data are shown as mean ± SD of 3–5 experiments per mutant cell line. **p < 0.005; ***p < 0.0005; ****p < 0.0001; two-way ANOVA. Mutants that significantly impact MOP activation are shown in red (K123A; K136A). Mutants that moderately impact MOP activation are shown in orange (K66A; S69A).

(C) Ribbon representation of the BTN3A1-IgV domain (yellow), with residues that impact MOP activation color coded as in (B) and residues that do not affect MOP activation shown in blue.

(D) Electrostatic nature of the patch on BTN3A1-IgV calculated with DelPhi. Positively charged residues are shown in blue and negatively charged residues in red, with the potential scale ranging from −7 (red) to +7 (blue) in units of kT/e.

(E) Molecular surface representation of the BTN3A1 ectodomain. Residues that affect P-Ag sensing by MOP TCR (red) in relation to 20.1 mAb (green) and 103.2 (orange) mAb binding sites are highlighted.

See also Figure S4.

BTN3A1-IgV/BTN2A1-IgV interaction is completely dispensable for P-Ag sensing. Moreover, they suggested that the ability of some BTN3A1-IgV mutations to abrogate P-Ag sensing operates independently of their effects on interaction with BTN2A1-IgV.

Identification of a molecular surface on BTN3A1-IgV critical for P-Ag sensing

In order to determine whether functionally abrogating mutations such as K136A represent part of a previously unrecognized wider recognition surface on BTN3A1-IgV, we selected BTN3A1-IgV residues as mutation candidates, focusing on residues relatively close to K136A and excluding those within the 20.1 mAb epitope since the MOP TCR we used for screening P-Ag reactivity is highly sensitive to 20.1 mAb-induced activation.[21] Additional criteria were surface accessibility and minimal/no involvement in intradomain stabilizing interaction networks that might compromise domain integrity upon alanine substitution. We then validated surface expression of mutant BTN3A1 and WT BTN2A1 in the CHO cell transduction system (Figures S4A and S4B) and tested the ability of individual mutant BTN3A1 molecules to support P-Ag sensing using the MOP TCR hybridoma (Figures 4A–4C). Some mutations had little effect

(Figures 4A–4C and S4C). In contrast, BTN3A1-IgV mutations K123A and K136A consistently abrogated P-Ag sensing, while K66A and S69A exhibited more subtle decreases in response (Figures 4A and 4B). These residues defined a contiguous patch on the CFG face of the BTN3A1-IgV domain (Figure 4C), which includes a distinctive positively charged surface (Figure 4D) that lies close to the footprint of the agonistic 20.1 mAb and is more distal to that of the inhibitory 103.2 mAb (Figure 4E). Collectively, these results establish the existence of a molecular surface on the BTN3A1-IgV domain that is critical for P-Ag sensing but operates independently from BTN3A1-IgV interactions with BTN2A1-IgV.

Analysis of the BTN3A1-linked proteome by immunoprecipitation

One possible explanation of these results is that following P-Ag exposure, BTN3A1, the P-Ag sensor, might associate via this surface patch on its membrane-distal IgV domain with a novel CDR3-recognized molecule and transport it into close association with BTN2A1 at the cell surface to form a P-Ag-induced composite ligand for the Vγ9Vδ2 TCR. To investigate this, we first carried out BTN3A1 immunoprecipitations following surface crosslinking of CHO cells expressing FLAG-tagged BTN3A1 and hemagglutinin (HA)-tagged BTN2A1, to identify potential association partners, both in the presence and absence of P-Ag. This approach was based on the observation that since human BTN3A1 and BTN2A1 successfully support P-Ag-mediated stimulation of human Vγ9Vδ2 TCR transductants when co-expressed in CHO cells,[7] they must retain any protein associations essential for Vγ9Vδ2 TCR interactions. Mass spectrometry analysis of BTN3A1-FLAG-associated proteins following SDS-PAGE and trypsinization identified many human BTN3A1 and BTN2A1 peptides, confirming a close interaction of these molecules in this transductant system. In addition, a modest range of endogenous hamster proteins were found to associate with BTN3A1-FLAG in the presence and absence of prior target cell Zol pretreatment (Figure S4D; Table S1), although among these, relatively few cell surface proteins were detected. Functional enrichment analysis of BTN3A1-associated proteins highlighted a diverse range of functions (Figure S4E), including ribosomal and proteasomal proteins and those involved in oxidative phosphorylation and carbon metabolism. Immunoprecipitation of HA-tagged BTN2A1 also identified many human BTN2A1 and BTN3A1 peptides (Figure S4F; Table S1), as well as yielded a smaller number of associated hamster proteins, also predominantly intracellular, that were similarly functionally diverse (Figure S4G). Although arguably no compelling candidates for a cell surface Vγ9Vδ2 TCR ligand were identified using either approach, several peptides from Chinese hamster BTN1A1 were identified in both experiments (Table S1). The involvement of BTN1A1 in P-Ag sensing was excluded using BTN1A1^{neg} HAP-1 cells, which activated JRT3 G115 TCR transductants as efficiently as WT HAP-1 cells (Figure S4H).

DISCUSSION

BTN2A1, recently established as a direct ligand for germline-encoded regions of the Vγ9 chain,[7,8] and BTN3A1,[6] the P-Ag sensor,[11] are highly functionally synergistic in P-Ag sensing[7,8]; however, the molecular explanation has remained unclear.[10] Recent studies have highlighted that P-Ag binding to the BTN3A1 B30.2 domain triggers association with BTN2A1 B30.2,[17,22] although they have left the nature of relevant extracellular changes unclear. Our results help clarify the nature of those recognition events and have implications for models that address how intracellular P-Ag exposure is coupled to TCR triggering.

Although studies that identified BTN2A1 highlighted overall proximity to BTN3A1 at the cell surface,[7,8] the additional finding that BTN2A1-IgV and BTN3A1-IgV directly associate with each other[7] raised the possibility that molecular association of the BTN3A1 and BTN2A1 ectodomains following intracellular P-Ag detection might be a critical component of the TCR-mediated sensing mechanism. While our findings establish a model for the BTN2A1-BTN3A1 ectodomain interaction that appears highly consistent with a viable, albeit weak (K_d >100 μM), cell surface interaction in *cis*, they ultimately demonstrate that the BTN2A1-IgV/BTN3A1-IgV complex is not a recognition target of the TCR. Not only is Vγ9Vδ2 TCR binding to BTN2A1 not enhanced by BTN2A1/BTN3A1 IgV-IgV interactions, but the two interactions are mutually exclusive due to overlapping interaction sites on BTN2A1. Therefore, the TCR and BTN3A1-IgV represent "either/or" binding partners for the BTN2A1-IgV domain, and the in *cis* BTN2A1-IgV:BTN3A1-IgV interaction shifts BTN2A1 into a TCR-inactive state. Moreover, functional experiments demonstrated that the BTN2A1-IgV/BTN3A1-IgV interaction itself was dispensable for P-Ag sensing. While this was initially surprising, particularly given the plausible nature of the predicted in *cis* association, the weak affinity of the BTN2A1-BTN3A1 ectodomain interaction suggests that such complexes are likely transient and unlikely to stably secure BTN2A1 in a TCR-inactive form. Consequently, there is likely no need to invoke mechanisms that actively "break" such interactions following P-Ag exposure. Nevertheless, a caveat is that BTN2A1 and BTN3A1 are overexpressed in the CHO cell functional assay system we used, and we cannot exclude the possibility that under physiological conditions, their ectodomain interaction may play a modulatory role, with two possibilities most likely. Firstly, by favoring close proximity of BTN2A1 and BTN3A dimers at the cell surface, such interactions might reduce the requirement for lateral diffusion following P-Ag binding to BTN3A1, thereby ensuring that P-Ag sensing proceeds with fast kinetics and with a potential for clustering adjacent signaling TCR complexes. Secondly, by temporarily locking BTN2A1-IgV in a "ground state" where it is unable to interact with the TCR, the BTN2A1-IgV/BTN3A1-IgV interaction might reduce the potential for basal signaling induced via BTN2A1/TCR interactions in the absence of antigen. Nevertheless, our results exclude the possibility that the BTN3A1-IgV/BTN2A1-IgV interaction is central to P-Ag sensing.

In contrast, our mutational experiments established the existence of an interaction surface on the CFG face of BTN3A1 IgV that is critical for TCR-dependent P-Ag sensing. Importantly, although this antigenic "hotspot" includes the K136 residue that does not affect the BTN2A1-IgV/BTN3A1-IgV interaction, it overlaps with the surface involved in interactions with BTN2A1,

and both regions involve the BTN3A1-IgV CFG face. In addition, we note that BTN3A1 K123 is within the hotspot and is predicted to be involved in interactions with BTN2A1-IgV in *cis*. Consequently, the BTN2A1-IgV/BTN3A1-IgV interaction in *cis* is likely not only to prevent TCR/BTN2A1 interactions but will also block the antigenic hotspot on BTN3A1-IgV from making additional interactions, albeit transiently. Moreover, as defined by our current mutagenesis dataset, the hotspot is distinct but adjacent to the epitope recognized by the highly potent 20.1 agonist mAb on BTN3A1.[23] It appears highly likely that recognition of this BTN3A1 CFG surface patch may explain involvement of regions on the Vγ9Vδ2 TCR that lie outside the germline-encoded BTN2A1 binding site on Vγ9 (including the HV4 region) and yet are implicated in P-Ag detection,[16] which include the CDR2δ loop and the clonotypically distinct CDR3δ and CDR3γ regions. However, we envisage at least two models whereby this could occur.

In model 1, BTN3A IgV is not recognized directly by the TCR, but instead its role is to position a novel ligand for direct TCR recognition. Although our mass spectroscopy experiments failed to identify a compelling candidate for such a ligand, caution should be exerted over their interpretation. We cannot exclude the possibility that such a ligand was below the level of detection or among the BTN3A1-associated proteins we identified. Interpretation is also complicated by the fact that a ligand could either associate constitutively with either BTN3A1 or BTN2A1 or could conceivably do so in a P-Ag-dependent fashion. However, in the absence of a compelling BTN3A1/BTN2A1-associated candidate ligand, model 2, whereby the TCR binds directly but weakly to BTN3A1/2-IgV, likely utilizing CDR2δ and clonotypically distinct CDR3 regions, warrants serious consideration. In addition, more complex models cannot be excluded (see limitations of the study).

Importantly, both models 1 and 2 can explain the immediate action of P-Ags, which sensitize target cells for recognition by Vγ9Vδ2 T cells extremely rapidly (10–90 s).[2] Also, either model could account for the strong agonistic activity of the 20.1 antibody since 20.1 action would result in clustering of a Vγ9Vδ2 TCR ligand in each case (model 1, via a BTN3A1-associated ligand; model 2, via BTN3A1 itself). However, model 2, likely involving direct interaction of additional TCR CDRs implicated in P-Ag sensing to the BTN3A1/2 CFG surface patch, more easily explains the observation that the 20.1 mAb, which binds adjacently, exhibits clonotype-specific effects on Vγ9Vδ2 T cell activation,[21] including Vγ9Vδ2 TCRs where 20.1 inhibits their activity—which could be rationalized by the binding mode of some Vγ9Vδ2 TCR clonotypes overlapping with that of the 20.1 mAb. Importantly, taking into account the P-Ag-driven association of BTN3A1 B30.2 with the BTN2A1-B30.2 domain,[17,22] neither model requires an "inside-out" transmission of conformational changes from the intracellular BTN3A1 B30.2 domain to the extracellular BTN2A1-IgV or BTN3A1-IgV domains specifically.[15,24] Indeed, our NMR data argue against a conformational change in either BTN2A1-IgV or the TCR following their interaction that favors subsequent BTN3A1 binding or indeed a conformational change in BTN3A1 induced by BTN2A1 binding that favors TCR interaction; moreover, we note that X-ray crystallographic studies of the BTN3A1 ectodomain revealed no substantial conformational differences in BTN3A1 IgV upon ligation by the 20.1 agonist mAb,[23] suggesting an obligatory conformational shift in BTN3A1 is unlikely.

Instead, both models we highlight represent distinct versions of a composite-ligand model whereby an extracellular-facing ligand fully licensed for TCR triggering is assembled from two nominally separate components, specifically BTN2A1 and BTN3A (with/without an associated ligand), by the action of P-Ag on their respective intracellular domains. While neither model invokes P-Ag-induced changes in BTN2A1-IgV or BTN3A1-IgV conformations, it is reasonable to assume that intracellular P-Ag-induced association of BTN3A1 B30.2 with BTN2A1 B30.2 may impose a specific relative orientation of both proteins' ectodomains (and potentially of those of partner proteins such as BTN3A2/A3) that could favor TCR interaction. Indeed, P-Ag-induced structural changes in BTN3A1 B30.2 alone appear insufficient to trigger inside-out signaling,[15] whereas a recent report from Yuan et al. does propose increased rigidification of the intracellular region of BTN3A1 following P-Ag-induced association with BTN2A1 B30.2 and fluctuations in the coiled-coil α-helical juxtamembrane regions that link B30.2 domains to the cell membrane,[22] which could conceivably affect the relative orientation of BTN3A1 and BTN2A1 ectodomains. Thus, the extracellularly focused composite-ligand model we support here may be broadly compatible with the intracellularly focused "molecular glue" model proposed by Yuan et al.[22] Of note, although our simplified experimental system deliberately excluded BTN3A2 and BTN3A3, BTN3A1 is known to readily form heterodimers with either of these isoforms.[25] In the context of such heterodimers, it is highly possible that the role of the BTN3A1 IgV domain evident in this study is in fact played in part or wholly by the N-terminal IgV domain of BTN3A2 and/or BTN3A3, which are identical and highly similar to that of BTN3A1, respectively. In this regard, our proposed model is also consistent with a recent study from Karunakaran and colleagues,[26] which examined the role of all BTN3A molecules and highlighted the importance of the BTN3A IgV domain in P-Ag sensing.

Two future experimental steps should be prioritized to delineate the two models we highlight. Although we defined the BTN3A1 CFG surface patch ("antigenic hotspot") in the context of the MOP TCR, extending this to a range of clonotypically distinct Vγ9Vδ2 TCRs would be highly informative (see limitations of the study). A distinct pattern of sensitivity to BTN3A1 mutants for each TCR would favor direct TCR recognition of the BTN3A1 recognition surface, whereas a highly consistent clonotypically independent pattern of recognition would favor the possibility that the BTN3A1 surface is not recognized directly but instead positions a conserved host-encoded component for TCR binding. Notably, in our previous study, mutagenesis of BTN3A1 R73 and Y127 affected recognition by expanded human Vγ9Vδ2 T cells, whereas these residues did not disrupt MOP TCR recognition in this study, suggestive of clonotypic differences.[20] Finally, in relation to this, a notable caveat of the current study is that we did not mutate the BTN3A1 domain exhaustively, and further mutagenesis would be informative to define the full extent of the functionally critical BTN3A1 CFG surface patch in the context of the MOP TCR and potentially other clonotypes.

Secondly, model 2 invokes direct interaction of the BTN3A1 extracellular domain with the Vγ9Vδ2 TCR. This has proven to be a highly contentious issue in the γδ T cell field, with a number of studies failing to detect direct interaction[11,14] following an initial report of binding by Vavassori et al.[27] In addition to convincingly refuting the apparent P-Ag binding to the IgV domain reported by Vavassori et al.,[27] Sandstrom et al. failed to replicate Vγ9Vδ2 TCR binding to BTN3A1 despite employing ligand multimers that were expected to detect interactions with affinities stronger than 500 μM.[11] In principle, although our NMR experiments could have detected direct BTN3A1-IgV/TCR interactions, they were limited to TCR concentrations of ~250 μM or less. Detectable line broadening would therefore not be expected if the K_d of the TCR/BTN3A1-IgV interaction was approaching the mM range. A caveat in this regard is that the recombinant proteins used in protein-protein binding assays may not accurately replicate the antigenic forms present *in vivo*, which could conceivably incorporate relevant post-translational modifications. However, the possibility remains that the physiological Vγ9Vδ2 TCR interaction with the BTN3A-IgV domain is extremely weak and yet, when coupled to the stronger TCR/BTN2A1-IgV interaction following P-Ag-induced association of BTN3A1 and BTN2A1 B30.2 domains, is sufficient to elicit TCR triggering. In support of this, the K_d of the Vγ9Vδ2 TCR/BTN2A1 interaction is 50 μM,[7,8] equivalent to weaker αβ TCR/pMHC interactions.[28] Thus, the P-Ag-sensing system may be finely poised to achieve TCR triggering by combining two energetically suboptimal TCR/ligand binding events in the presence of antigen. Taking these points into consideration, and in light of the lack of compelling novel BTN3A1/BTN2A1-associated candidate TCR ligands from our immunoprecipitation experiments, validation of model 2 as a preferred P-Ag-sensing mechanism is a high priority. This will depend on the generation of a robust dataset that firmly establishes direct, albeit likely weak, Vγ9Vδ2 TCR interactions with BTN3A-IgV, ideally clarifying the involvement of CDR regions implicated in P-Ag recognition but not involved in TCR/BTN2A1 interactions, in such binding events. Conceivably, such efforts could include methods that constrain binding to two dimensions, which might provide a more physiological and sensitive approach to assess relevant interactions.

Limitations of the study

Our study has three principle limitations. Firstly, our use of rodent cell lines (CHO and mouse 53/4 hybridoma cells) as BTN2A1-/BTN3A-expressing target cells and effector cells should be noted. Comparisons with human systems are warranted; however, since essential elements of the P-Ag-sensing process are preserved in this context, critical mechanistic elements related to our conclusions are likely conserved. Unfortunately, since 53/4 hybridomas expressing other Vγ9Vδ2 TCR clonotypes we tested were not activated by BTN2A1-/BTN3A1-expressing CHO cells exposed to P-Ag/20.1 mAb, determining the influence of Vγ9Vδ2 TCR clonotype on differences in recognition of the BTN3A1 surface patch was not possible. Future studies to address this question will therefore be best directed at different cellular systems. Secondly, to simplify experimental interpretation, we employed a simplified approach that combined expression of BTN2A1 with solely the BTN3A1 isoform and excluded the BTN3A2 and BTN3A3 isoforms. Especially since the BTN3A2 IgV domain is identical to that of BTN3A1, we therefore cannot exclude the possibility that in the context of a physiological system, TCR-mediated recognition of the BTN3A-IgV patch may partly or chiefly involve other isoforms (i.e., 3A2/3A3), a possibility that subsequent studies should address. Thirdly, our results do not exclude the possibility that the BTN3A1 surface we have defined might directly engage a currently unidentified (i.e., non-TCR) ligand on the T cell surface as part of the P-Ag-sensing mechanism.[29] This model is arguably more complex than those discussed above, as it would need to invoke an additional TCR ligand on the target cell to account for established involvement of TCR regions outside of those involved in BTN2A1 interaction.

STAR★METHODS

Detailed methods are provided in the online version of this paper and include the following:

- KEY RESOURCES TABLE
- RESOURCE AVAILABILITY
  - Lead contact
  - Materials availability
  - Data and code availability
- EXPERIMENTAL MODEL AND SUBJECT DETAILS
- METHOD DETAILS
  - Generation of FLAG/HA tagged BTN3A1 and BTN2A1, and BTN3A1 mutants
  - CHO cell transduction and CHO assays
  - Soluble protein production
  - Flow cytometry
  - Surface crosslinking, immunoprecipitation, mass spectroscopy, and functional enrichment analysis
  - Modelling the BTN2A1-IgV/Vγ9 and BTN2A1-BTN3A1-IgV complexes
  - NMR
  - Software
- QUANTIFICATION AND STATISTICAL ANALYSIS

SUPPLEMENTAL INFORMATION

Supplemental information can be found online at https://doi.org/10.1016/j.celrep.2023.112321.

ACKNOWLEDGMENTS

This work was supported by the Wellcome Trust, UK (grant 221725/Z/20/Z to B.E.W. supporting C.R.W., M.S., and F.M.) and by a Midlands Integrative Biosciences Training Partnership PhD studentship to C.R.B. NMR studies were supported by a Wellcome Trust Biomedical Resources grant 208400/Z/17/Z, and we thank HWB-NMR staff at the University of Birmingham for providing open access to their Wellcome Trust-funded 800 MHz NMR spectrometer. M.M.K. and T.H. were supported by German Research Foundation (DFG) HE2346/8-2 within FOR 2799 "Receiving and Translating Signals" via the γδ T cell receptor, awarded to T.H. We thank the University of Birmingham Protein Expression Facility for use of their equipment; Dr. Jinglei Yu at the Advanced Mass Spectroscopy Facility, School of Biosciences, University of Birmingham, for specialist advice; and Thomas Winkler for the recombinant BTN2A1 antibody.

AUTHOR CONTRIBUTIONS

Conceptualization, C.R.W., M.S., M.J., and B.E.W.; methodology, C.R.W., M.S., M.M.K., T.H., M.J., and B.E.W.; investigation, C.R.W., M.S., C.R.B., M.M.K., E.J.E., C.v.K., K.A.B., and M.J.; writing – original draft, C.R.W. and B.E.W.; writing – review & editing, C.R.W., T.H., M.J., and B.E.W.; visualization: C.R.W., M.M.K., T.H., F.M., M.J., and B.E.W.; funding acquisition, B.E.W.; resources, T.H.

DECLARATION OF INTERESTS

B.E.W. provides consultancy regarding the development of γδ T cell immunotherapy approaches for Ferring Ventures SA, linked to Ferring Pharmaceuticals.

INCLUSION AND DIVERSITY

We support inclusive, diverse, and equitable conduct of research.

Received: October 20, 2022
Revised: February 21, 2023
Accepted: March 15, 2023
Published: March 28, 2023

REFERENCES

1. Karunakaran, M.M., and Herrmann, T. (2014). The Vgamma9Vdelta2 T cell antigen receptor and butyrophilin-3 A1: models of interaction, the possibility of co-evolution, and the case of dendritic epidermal T cells. Front. Immunol. *5*, 648. https://doi.org/10.3389/fimmu.2014.00648.
2. Morita, C.T., Jin, C., Sarikonda, G., and Wang, H. (2007). Nonpeptide antigens, presentation mechanisms, and immunological memory of human Vgamma2Vdelta2 T cells: discriminating friend from foe through the recognition of prenyl pyrophosphate antigens. Immunol. Rev. *215*, 59–76. https://doi.org/10.1111/j.1600-065X.2006.00479.x.
3. Hintz, M., Reichenberg, A., Altincicek, B., Bahr, U., Gschwind, R.M., Kollas, A.K., Beck, E., Wiesner, J., Eberl, M., and Jomaa, H. (2001). Identification of (E)-4-hydroxy-3-methyl-but-2-enyl pyrophosphate as a major activator for human gammadelta T cells in Escherichia coli. FEBS Lett. *509*, 317–322. https://doi.org/10.1016/s0014-5793(01)03191-x.
4. Mulani, M.S., Kamble, E.E., Kumkar, S.N., Tawre, M.S., and Pardesi, K.R. (2019). Emerging strategies to combat ESKAPE pathogens in the era of antimicrobial resistance: a review. Front. Microbiol. *10*, 539. https://doi.org/10.3389/fmicb.2019.00539.
5. Junqueira, C., Polidoro, R.B., Castro, G., Absalon, S., Liang, Z., Sen Santara, S., Crespo, Â., Pereira, D.B., Gazzinelli, R.T., Dvorin, J.D., and Lieberman, J. (2021). Gammadelta T cells suppress Plasmodium falciparum blood-stage infection by direct killing and phagocytosis. Nat. Immunol. *22*, 347–357. https://doi.org/10.1038/s41590-020-00847-4.
6. Harly, C., Guillaume, Y., Nedellec, S., Peigné, C.M., Mönkkönen, H., Mönkkönen, J., Li, J., Kuball, J., Adams, E.J., Netzer, S., et al. (2012). Key implication of CD277/butyrophilin-3 (BTN3A) in cellular stress sensing by a major human gammadelta T-cell subset. Blood *120*, 2269–2279. https://doi.org/10.1182/blood-2012-05-430470.
7. Karunakaran, M.M., Willcox, C.R., Salim, M., Paletta, D., Fichtner, A.S., Noll, A., Starick, L., Nöhren, A., Begley, C.R., Berwick, K.A., et al. (2020). Butyrophilin-2A1 directly binds germline-encoded regions of the Vgamma9Vdelta2 TCR and is essential for phosphoantigen sensing. Immunity *52*, 487–498.e6. https://doi.org/10.1016/j.immuni.2020.02.014.
8. Rigau, M., Ostrouska, S., Fulford, T.S., Johnson, D.N., Woods, K., Ruan, Z., McWilliam, H.E.G., Hudson, C., Tutuka, C., Wheatley, A.K., et al. (2020). Butyrophilin 2A1 is essential for phosphoantigen reactivity by gammadelta T cells. Science *367*, eaay5516. https://doi.org/10.1126/science.aay5516.
9. Willcox, B.E., and Willcox, C.R. (2019). Gammadelta TCR ligands: the quest to solve a 500-million-year-old mystery. Nat. Immunol. *20*, 121–128. https://doi.org/10.1038/s41590-018-0304-y.
10. Willcox, C.R., Mohammed, F., and Willcox, B.E. (2020). The distinct MHC-unrestricted immunobiology of innate-like and adaptive-like human gammadelta T cell subsets-Nature's CAR-T cells. Immunol. Rev. *298*, 25–46. https://doi.org/10.1111/imr.12928.
11. Sandstrom, A., Peigné, C.M., Léger, A., Crooks, J.E., Konczak, F., Gesnel, M.C., Breathnach, R., Bonneville, M., Scotet, E., and Adams, E.J. (2014). The intracellular B30.2 domain of butyrophilin 3A1 binds phosphoantigens to mediate activation of human Vgamma9Vdelta2 T cells. Immunity *40*, 490–500. https://doi.org/10.1016/j.immuni.2014.03.003.
12. Davey, M.S., Malde, R., Mykura, R.C., Baker, A.T., Taher, T.E., Le Duff, C.S., Willcox, B.E., and Mehellou, Y. (2018). Synthesis and biological evaluation of (E)-4-Hydroxy-3-methylbut-2-enyl phosphate (HMBP) aryloxy triester phosphoramidate prodrugs as activators of Vgamma9/Vdelta2 T-cell immune responses. J. Med. Chem. *61*, 2111–2117. https://doi.org/10.1021/acs.jmedchem.7b01824.
13. Hsiao, C.H.C., Lin, X., Barney, R.J., Shippy, R.R., Li, J., Vinogradova, O., Wiemer, D.F., and Wiemer, A.J. (2014). Synthesis of a phosphoantigen prodrug that potently activates Vgamma9Vdelta2 T-lymphocytes. Chem. Biol. *21*, 945–954. https://doi.org/10.1016/j.chembiol.2014.06.006.
14. Salim, M., Knowles, T.J., Baker, A.T., Davey, M.S., Jeeves, M., Sridhar, P., Wilkie, J., Willcox, C.R., Kadri, H., Taher, T.E., et al. (2017). BTN3A1 discriminates gammadelta T cell phosphoantigens from nonantigenic small molecules via a conformational sensor in its B30.2 domain. ACS Chem. Biol. *12*, 2631–2643. https://doi.org/10.1021/acschembio.7b00694.
15. Yang, Y., Li, L., Yuan, L., Zhou, X., Duan, J., Xiao, H., Cai, N., Han, S., Ma, X., Liu, W., et al. (2019). A structural change in butyrophilin upon phosphoantigen binding underlies phosphoantigen-mediated Vgamma9Vdelta2 T cell activation. Immunity *50*, 1043–1053.e5. https://doi.org/10.1016/j.immuni.2019.02.016.
16. Wang, H., Fang, Z., and Morita, C.T. (2010). Vgamma2Vdelta2 T Cell Receptor recognition of prenyl pyrophosphates is dependent on all CDRs. J. Immunol. *184*, 6209–6222. https://doi.org/10.4049/jimmunol.1000231.
17. Hsiao, C.H.C., Nguyen, K., Jin, Y., Vinogradova, O., and Wiemer, A.J. (2022). Ligand-induced interactions between butyrophilin 2A1 and 3A1 internal domains in the HMBPP receptor complex. Cell Chem. Biol. *29*, 985–995.e5. https://doi.org/10.1016/j.chembiol.2022.01.004.
18. Honorato, R.V., Koukos, P.I., Jiménez-García, B., Tsaregorodtsev, A., Verlato, M., Giachetti, A., Rosato, A., and Bonvin, A.M.J.J. (2021). Structural biology in the clouds: the WeNMR-EOSC ecosystem. Front. Mol. Biosci. *8*, 729513. https://doi.org/10.3389/fmolb.2021.729513.
19. van Zundert, G.C.P., Rodrigues, J.P.G.L.M., Trellet, M., Schmitz, C., Kastritis, P.L., Karaca, E., Melquiond, A.S.J., van Dijk, M., de Vries, S.J., and Bonvin, A.M.J.J. (2016). The HADDOCK2.2 web server: user-friendly integrative modeling of biomolecular complexes. J. Mol. Biol. *428*, 720–725. https://doi.org/10.1016/j.jmb.2015.09.014.
20. Willcox, C.R., Vantourout, P., Salim, M., Zlatareva, I., Melandri, D., Zanardo, L., George, R., Kjaer, S., Jeeves, M., Mohammed, F., et al. (2019). Butyrophilin-like 3 directly binds a human Vgamma4(+) T cell receptor using a modality distinct from clonally-restricted antigen. Immunity *51*, 813–825.e4. https://doi.org/10.1016/j.immuni.2019.09.006.
21. Starick, L., Riano, F., Karunakaran, M.M., Kunzmann, V., Li, J., Kreiss, M., Amslinger, S., Scotet, E., Olive, D., De Libero, G., and Herrmann, T. (2017). Butyrophilin 3A (BTN3A, CD277)-specific antibody 20.1 differentially activates Vgamma9Vdelta2 TCR clonotypes and interferes with phosphoantigen activation. Eur. J. Immunol. *47*, 982–992. https://doi.org/10.1002/eji.201646818.
22. Yuan, L., Ma, X., Yang, Y., Li, X., Ma, W., Yang, H., Huang, J.-W., Xue, J., Yi, S., Zhang, M., et al. (2023). Phosphoantigens are molecular glues that promote butyrophilin 3A1/2A1 association leading to Vγ9Vδ2 T cell activation. Preprint at bioRxiv. https://doi.org/10.1101/2022.01.02.474068v1.

23. Palakodeti, A., Sandstrom, A., Sundaresan, L., Harly, C., Nedellec, S., Olive, D., Scotet, E., Bonneville, M., and Adams, E.J. (2012). The molecular basis for modulation of human Vgamma9Vdelta2 T cell responses by CD277/butyrophilin-3 (BTN3A)-specific antibodies. J. Biol. Chem. *287*, 32780–32790. https://doi.org/10.1074/jbc.M112.384354.

24. Gu, S., Sachleben, J.R., Boughter, C.T., Nawrocka, W.I., Borowska, M.T., Tarrasch, J.T., Skiniotis, G., Roux, B., and Adams, E.J. (2017). Phosphoantigen-induced conformational change of butyrophilin 3A1 (BTN3A1) and its implication on Vgamma9Vdelta2 T cell activation. Proc. Natl. Acad. Sci. USA *114*, E7311–E7320. https://doi.org/10.1073/pnas.1707547114.

25. Vantourout, P., Laing, A., Woodward, M.J., Zlatareva, I., Apolonia, L., Jones, A.W., Snijders, A.P., Malim, M.H., and Hayday, A.C. (2018). Heteromeric interactions regulate butyrophilin (BTN) and BTN-like molecules governing gammadelta T cell biology. Proc. Natl. Acad. Sci. USA *115*, 1039–1044. https://doi.org/10.1073/pnas.1701237115.

26. Karunakaran, M.M., Subramanian, H., Jin, Y., Mohammed, F., Kimmel, B., Juraske, C., Starick, L., Nöhren, A., Länder, N., Willcox, C.R., et al. (2023). Division of labor and cooperation between different butyrophilin proteins controls phosphoantigen-mediated activation of human γδ T cells. Res. Sq. https://doi.org/10.21203/rs.3.rs-2583246/v1.

27. Vavassori, S., Kumar, A., Wan, G.S., Ramanjaneyulu, G.S., Cavallari, M., El Daker, S., Beddoe, T., Theodossis, A., Williams, N.K., Gostick, E., et al. (2013). Butyrophilin 3A1 binds phosphorylated antigens and stimulates human gammadelta T cells. Nat. Immunol. *14*, 908–916. https://doi.org/10.1038/ni.2665.

28. Davis, M.M., Boniface, J.J., Reich, Z., Lyons, D., Hampl, J., Arden, B., and Chien, Y. (1998). Ligand recognition by alpha beta T cell receptors. Annu. Rev. Immunol. *16*, 523–544. https://doi.org/10.1146/annurev.immunol.16.1.523.

29. Vyborova, A., Beringer, D.X., Fasci, D., Karaiskaki, F., van Diest, E., Kramer, L., de Haas, A., Sanders, J., Janssen, A., Straetemans, T., et al. (2020). gamma9delta2T cell diversity and the receptor interface with tumor cells. J. Clin. Invest. *130*, 4637–4651. https://doi.org/10.1172/JCI132489.

30. Li, L., Li, C., Sarkar, S., Zhang, J., Witham, S., Zhang, Z., Wang, L., Smith, N., Petukh, M., and Alexov, E. (2012). DelPhi: a comprehensive suite for DelPhi software and associated resources. BMC Biophys. *5*, 9. https://doi.org/10.1186/2046-1682-5-9.

31. Li, C., Jia, Z., Chakravorty, A., Pahari, S., Peng, Y., Basu, S., Koirala, M., Panday, S.K., Petukh, M., Li, L., and Alexov, E. (2019). DelPhi suite: new developments and review of functionalities. J. Comput. Chem. *40*, 2502–2508. https://doi.org/10.1002/jcc.26006.

32. Willcox, C.R., Pitard, V., Netzer, S., Couzi, L., Salim, M., Silberzahn, T., Moreau, J.F., Hayday, A.C., Willcox, B.E., and Déchanet-Merville, J. (2012). Cytomegalovirus and tumor stress surveillance by binding of a human gammadelta T cell antigen receptor to endothelial protein C receptor. Nat. Immunol. *13*, 872–879. https://doi.org/10.1038/ni.2394.

33. Sherman, B.T., Hao, M., Qiu, J., Jiao, X., Baseler, M.W., Lane, H.C., Imamichi, T., and Chang, W. (2022). DAVID: a web server for functional enrichment analysis and functional annotation of gene lists (2021 update). Nucleic Acids Res. *50*, W216–W221. https://doi.org/10.1093/nar/gkac194.

34. Vranken, W.F., Boucher, W., Stevens, T.J., Fogh, R.H., Pajon, A., Llinas, M., Ulrich, E.L., Markley, J.L., Ionides, J., and Laue, E.D. (2005). The CCPN data model for NMR spectroscopy: development of a software pipeline. Proteins *59*, 687–696. https://doi.org/10.1002/prot.20449.

STAR★METHODS

KEY RESOURCES TABLE

REAGENT or RESOURCE	SOURCE	IDENTIFIER
Antibodies		
Anti-huBTN3 (CD277) clone 20.1	Invitrogen	Cat#14-2779-82; RRID: AB_467550
Anti-huBTN2A1	Gift from Prof Thomas Winkler	N/A
Anti-HA.11 epitope tag affinity matrix (clone 16B12)	Biolegend	Cat#900801; RRID: AB_2564999
Purified anti-DYKDDDDK (FLAG) tag antibody (clone L5)	Biolegend	Cat#637302; RRID: AB_1134268
Anti-DYKDDDDK (FLAG) tag affinity matrix (clone L5)	Biolegend	Cat#651502; RRID: AB_10959657
Goat anti-mouse FITC	Sigma	Cat#F0257; RRID: AB_259378
Bacterial and virus strains		
NEB 5-alpha	NEB	Cat# C2987H
BL21 (DE3)	NEB	Cat# C2527H
Chemicals, peptides, and recombinant proteins		
HMBPP	Sigma	Cat#95098
Zoledronate	Sigma	Cat#SML0223
NdeI	Roche	Cat# 11 040 227 001
BamHI	Roche	Cat# 10 567 604 001
BTN2A1 IgV and mutants	(Karunakaran et al.[7]) and this study	N/A
BTN3A1 IgV and mutants	(Salim et al.[14]) and this study	N/A
Sulfo-EGS crosslinker	ThermoFisher Scientific	Cat#21566
Soluble G115 TCR produced in drosophila cells	(Karunakaran et al.[7])	N/A
Critical commercial assays		
IL-2 mouse uncoated ELISA kit	Invitrogen	Cat #88-7024-88
QuikChange II XL site directed mutagenesis kit	Agilent	Cat#200521-5
Experimental models: Cell lines		
293T	ECACC	12022001; RRID: CVCL_0063
CHO (CHO-K1) expressing rm CD80, BTN2A1 and BTN3A1	(Starick et al.[21])	N/A
53/4 hybridoma expressing MOP Vγ9Vδ2 TCR	(Starick et al.[21])	N/A
HAP-1 parental cell line	Horizon	C631; RRID: CVCL_Y019
HAP-1 BTN1A1-deficient cell line	Horizon	HZGHC008003c012
Oligonucleotides		
For site directed mutagenesis primers, please see Table S2		N/A
Recombinant DNA		
pIZ	Gift from Dr. Ingolf Berberich	N/A
pIH	Gift from Dr. Ingolf Berberich	N/A
pIH-FLAG	(Karunakaran et al.[7])	N/A
pET23a	Merck Millipore	Cat# 69745-3

(*Continued on next page*)

Continued

REAGENT or RESOURCE	SOURCE	IDENTIFIER
BTN2A1 IgV in pET23a (wild type and mutants)	This paper	N/A
BTN3A1 IgV in pET23a (wild type and mutants)	(Salim et al.[14])	N/A
Software and algorithms		
FlowJo version 10	FlowJo LLC	https://www.flowjo.com/
PyMOL version 2.0.7	Schrodinger LLC	https://pymol.org
GraphPad Prism version 9.2	GraphPad Software LLC	https://www.graphpad.com
HADDOCK	(Honorato et al.[18]; van Zundert et al.[19])	https://wenmr.science.uu.nl/haddock2.4/
DelPhi	(Li et al.[30]; Li et al.[31])	http://honig.c2b2.columbia.edu/delphi

RESOURCE AVAILABILITY

Lead contact

Further information and requests for reagents and data will be addressed by the lead contact, Benjamin Willcox (b.willcox@bham.ac.uk).

Materials availability

All reagents and resources generated in this study are available on request from the lead contact.

Data and code availability

- Data reported in this paper are available from the lead contact upon request.
- This paper does not report original code.
- Any additional information required to reanalyze the data reported in this paper is available from the lead contact upon request.

EXPERIMENTAL MODEL AND SUBJECT DETAILS

CHO cells and 53/4 hybridoma TCR transductants were cultured in RPMI (Sigma) supplemented with 10% Foetal Bovine Serum (FBS), 1 mM sodium pyruvate, 2 mM glutamine, 0.1 mM nonessential amino acids, 5 mM β-mercaptoethanol, penicillin (100 U/mL) and streptomycin (100 U/mL). JRT3 cells expressing the G115 TCR were cultured in RPMI supplemented with 10% FBS, 0.1 mM nonessential amino acids, and pen/strep. WT and BTN1A1-deficient HAP1 cells were cultured in IMDM (Thermo) supplemented with 10% FBS and pen/strep.

METHOD DETAILS

Generation of FLAG/HA tagged BTN3A1 and BTN2A1, and BTN3A1 mutants

Generation of BTN3A1 incorporating an N-terminal FLAG tag in pIH, and BTN2A1 incorporating a C-terminal HA-tag in pIZ, were previously described.[7] BTN3A1 mutants were generated by site-directed mutagenesis of FLAG-BTN3A1/pIHusing the QuikChange II XL kit (Stratagene), following manufacturer's instructions, using the primers in Table S2.

CHO cell transduction and CHO assays

CHO cells previously transduced with rat/mouse CD80 and human BTN2A1[7] were additionally transduced with pIH vector encoding WT or mutant BTN3A1 as previously described.[21] CHO cells expressing rmCD80, WT BTN2A1 and WT or mutant BTN3A1 (10^4/well) were plated in 96 well plates in duplicate and incubated overnight. CHO cells were then pulsed with HMBPP (0–10μM final concentration) and 53/4 hybridoma cells expressing the MOP TCR[7] were added (5×10^4) and incubated at 37°C for 16hr. Supernatants were removed and analysed by ELISA for mouse IL-2.[7]

Soluble protein production

cDNA encoding WT BTN2A1-IgV (S27 to V142), BTN3A1-IgV (S28-V143) or BTN2A1 or BTN3A1 IgV incorporating the described mutations, were generated as gblocks (Integrated DNA Technologies) including the sequence for a C-terminal 6x Histidine tag and cloned into the pET23a expression vector (Novagen). Proteins were overexpressed, purified and refolded as described.[7,20] WT and mutant BTN2A1 IgV domains were refolded by dilution in 100 mM Tris, 400 mM L-Arginine-HCl, 2 mM EDTA, 6.8 mM cystamine, 2.7 mM cysteamine, 0.1 mM PMSF, pH 8, overnight at 4°C. The refolding mixture was concentrated and purified by size exclusion

chromatography on a Superdex-200 column (GE Healthcare) pre-equilibrated with 20 mM Tris, 150 mM NaCl, pH 8, or 20 mM Na_3PO_4 pH 7.4, 50mM NaCl buffer. BTN3A1-IgV was expressed, refolded, and purified as described.[14] Soluble G115 Vγ9Vδ2 TCR was generated in Drosophila S2 cells and purified by nickel chromatography as previously described.[7,32]

Flow cytometry

The expression of BTN3A1 and BTN2A1 were detected with anti-DYKDDDDK (FLAG; Biolegend), anti-huBTN3 (CD277) clone 20.1 (Thermo) or recombinant anti-huBTN2A1 (gift of Thomas Winkler), followed by secondary antibody F(ab') goat anti mouse IgG (H+L) FITC (Sigma). Samples were analysed on an LSRII flow cytometer (BD).

Surface crosslinking, immunoprecipitation, mass spectroscopy, and functional enrichment analysis

CHO cells overexpressing HA-tagged BTN2A1 and FLAG-tagged BTN3A1 were treated with 20 μM Zoledronate overnight. They were then treated with the soluble, membrane-impermeable crosslinker sulfo-EGS (ThermoFisher) (0.5mM in PBS), at 4°C for 2 hours. Following this, the reaction was quenched by addition of Tris pH 7.5 to a final concentration of 20mM. Cells were washed in TBS and lysed in 1% NP40 in TBS lysis buffer. After centrifugation to remove insoluble material, immunoprecipitation was carried out using anti-HA resin or anti-FLAG resin. Immunoprecipitations were washed in lysis buffer and eluted in nonreducing (NR) SDS sample buffer before running for 1cm on 4–20% SDS-PAGE gels (BioRad). Bands were detected using Coomassie Blue and excised from the gel, and mass spec analysis was carried out by Functional Genomics Birmingham. Initial mass spectroscopy peptide hits were identified with by searching the *Cricetulus griseus* genome PICRH assembly (https://blast.chogenome.org/archive/Genomes/C_griseus/CH-PICRH/current/annotations/RefSeq_072020/GCF_003668045.3_CriGri-PICRH-1.0_protein.faa.gz). Subsequent functional annotation and enrichment analysis of BTN3A1-associated and BTN2A1-associated *C. griseus* gene lists was carried out using the Database for Annotation, Visualisation and Integrated Discovery (DAVID).[33] Functional annotation clustering was based on Gene Ontology (GO terms biological process, cellular compartment, molecular function), and Pathway analysis (KEGG Pathway). Select pathways/GO-terms from each annotation cluster are shown in Figures S4E and S4G.

Modelling the BTN2A1-IgV/Vγ9 and BTN2A1-BTN3A1-IgV complexes

The model of the BTN2A1-IgV/Vγ9 complex was generated as described previously.[7] BTN2A1-IgV/BTN3A1-IgV complex was modelled with HADDOCK.[19] BTN2A1 residues (63, 67, 72, 74, 78, 79, 81, 82, 83 and 86) were classified as active in Vγ9 binding based upon NMR binding experiments. 'Passively involved' residues were selected automatically. BTN3A1 residues (53, 68, 69, 134, 135, 136, 137, 138) selected for use as ambiguous interaction restraints to drive the docking process with BTN2A1 were also derived from NMR binding experiments.

NMR

HSQC experiments were performed at 298K on either a 600MHz Bruker Avance III or 800MHz Bruker Neo spectrometer equipped with a 1.7 mm TCI cryogenically cooled triple resonance probe. Protein concentrations used were as stated and the final volume used was 35 μL. Data were collected using an echo-antiecho HSQC sequence using an inter-scan delay of 1.5 seconds. Data were acquired using a sweep width of 16 ppm and 2048 complex data points in the ^{1}H dimension with 35 ppm and 256 increments in the ^{15}N dimension. Experiments were processed using Topspin (Bruker). All analysis was performed using CCPN Analysis.[34]

Software

Structural figures were generated in PyMOL (version 2.0.7; Schrodinger, LLC), with the electrostatic surface potential of the BTN3A1-IgV calculated using Delphi.[30,31] Graphs were generated in Excel or GraphPad Prism v9.2.

QUANTIFICATION AND STATISTICAL ANALYSIS

Differences between IL-2 production in response to CHO cells expressing WT or mutant BTN3A1 were analysed using Mann-Whitney test or two-way ANOVA.